

# DISLOCATION MODELLING OF LOCALIZED PLASTICITY IN PERSISTENT SLIP BANDS

Jaafar A. El-Awady<sup>1</sup>, Nasr M. Ghoniem<sup>1</sup>, Hael Mughrabi<sup>2</sup>

<sup>1</sup>Mechanical and Aerospace Engineering Department, University of California, Los Angeles  
(UCLA), CA 90095-1597, USA

<sup>2</sup>Institut für Werkstoffwissenschaften, Allgemeine Werkstoffeigenschaften, Universität  
Melanogen-Nüenrober Magenstrasse 5, D-91058 Melanogen, Germany

Keywords: Persistent Slip Bands, Dislocation Dynamics, Fatigue Saturation Stress.

## Abstract

We present models of localized plastic deformation inside Persistent Slip Band channels. First, we investigate the interaction between screw dislocations as they pass one another inside channel walls in copper. The model shows the mechanisms of dislocation bowing, dipole formation and binding, and finally dipole destruction as screw dislocations pass one another. The mechanism of (dipole passing) is assessed and interpreted in terms of the fatigue saturation stress. We also present results for the effects of the wall dipole structure on the dipole passing mechanism.

## Introduction

A common ingredient in the models of fatigue crack nucleation is the existence of irreversible slip, caused by the progressive interaction of Persistent Slip Bands (PSBs) with the material surface resulting in concentration of the plastic displacement. A widely accepted model of PSBs is the Essman-Gösele-Mughrabi (EGM) extrusion theory [1], where they propose a semi-quantitative theory of the evolution of the surface profile of PSBs in fatigued metals on the basis of bulk dislocation processes. The essential features of this theory is the annihilation of pairs of both screw and edge dislocations, which leads to irreversible slip. Moreover, this theory suggests that extrusions form in a rapid manner as a result of the combined effect of dislocation glide and annihilation of close dipoles. Due to this latter effect, the mean glide plane becomes slightly inclined to the crystallographic glide plane, and edge dislocations of opposite sign are deposited on the two PSB-matrix interfaces.

There are a number of factors that contribute to the saturation fatigue stress (or fatigue limit) in pure metals, and these are [2, 3]: (i) the stress required to allow two screw dislocations of opposite signs on parallel slip planes to pass one another, (ii) the stress required for bowing of screw dislocations in between PSB walls, and (iii) the long range internal stress field resulting from edge dislocation dipolar walls. To understand the influence of these mechanisms on the fatigue limit, a number of papers have been published on the glide of dislocations in PSBs [3 - 9].

Grosskreutz and Mughrabi [4] made an approximate estimate for the passing stress as a linear superposition of the screw dipole passing stress and the critical Orowan bowing stress for screw dislocations gliding inside dipolar PSB walls. This estimate was then adopted

by Brown [5, 6], who studied the problem of two rigid screw dislocations, of opposite sign, passing one another and depositing edge dislocations on the two dipolar walls that confine them. Brown [5] deduced that the passing stress must be equal to the dipole passing stress, and that the two should be added together. Mughrabi and Pschenitzka [7] modified this conclusion by considering two elliptical screw dislocations confined between the walls. They predicted that the passing stress is not a direct addition of the bowing stress and the dipole passing stress but instead is about 20% larger than either one. Thus, they predicted that the linear superposition gives about 70-80% overestimate (i.e. only about 20% of the Orowan bowing stress adds to the passing stress). In response, Brown [3] presented a modified estimate in which the passing stress is computed as the sum of the bowing stress and the passing stress reduced from that for infinite straight screws. In this work, Brown concludes that about 50% of the Orowan bowing stress adds to the passing stress (40-70% when suitable parameters are chosen). Because of this wide range of conclusions obtained from analytical models of the fatigue saturation stress, the need for computer models based on numerical techniques is essential for accurate predictions.

Discrete Dislocation Dynamics (DDD) has been developed in the last decade for fundamental descriptions of plasticity and fracture at the meso-scale. The approach relies on direct numerical simulations of the collective motion of dislocation ensembles without ad hoc assumptions by direct numerical solution of the equations of motion. This approach has been successfully used in many applications at the nano- and micro-scales [10 - 13]. In this paper, we explore, through the use of the DDD method, the effect of the shape of the screw dislocations as they simultaneously bow between the walls and pass one another on the passing stress. In addition, the effect of the long range internal stress field resulting from edge dislocation dipolar walls on the passing stress is investigated.

Recently, Schwarz and Mughrabi [8] and Křišť'an and Kratochvíl [9] used the DDD method to provide additional insight into the PSB problem. Although, the details of the present model are different from those of references [8, 9], the results will be shown to be comparable. In the work of Schwarz and Mughrabi [8], dislocations are confined in a channel and are modelled as short straight dislocations. In the study of Křišť'an and Kratochvíl [9], dislocations are modelled as planar flexible curves confined by an infinitely long edge dipole on each side (i.e the PSB wall is represented by a single dipole on each side). Also, for their calculation of the bowing stress, they use the line tension approximation. In the present investigation, we model the screw dislocations as curved parametric segments [14]. The screw dislocations are confined either by an infinitely long edge dipole on each side, or by a more realistic case of a high density dipolar wall. Self-forces are computed following the method of Gavazza and Barnett [15], as discussed in reference [13].

In this paper, first we first present details of our model. We then we present the numerical results of the fatigue saturation stress and investigate the interaction between screw dislocations as they pass one another inside PSB channels in copper. We then discuss the role of additional factors on the passing stress including the internal stress resulting from the resistance to plastic flow of the walls being much greater than that of the inter-wall material, the slip plane spacing, and the channel width.

## Computational Model

The glide and interaction of screw dislocations in PSB channel walls of densely-packed edge dislocation dipoles is considered. Referring to the structure of a PSB, consider a crystal having a channel in which two screw dislocations of opposite sign glide towards each other, extending from one side to the other, i.e. with Burgers vector perpendicular to the two bounding interfaces (walls). This problem will be considered and approximated by the two models shown in Figure 1.

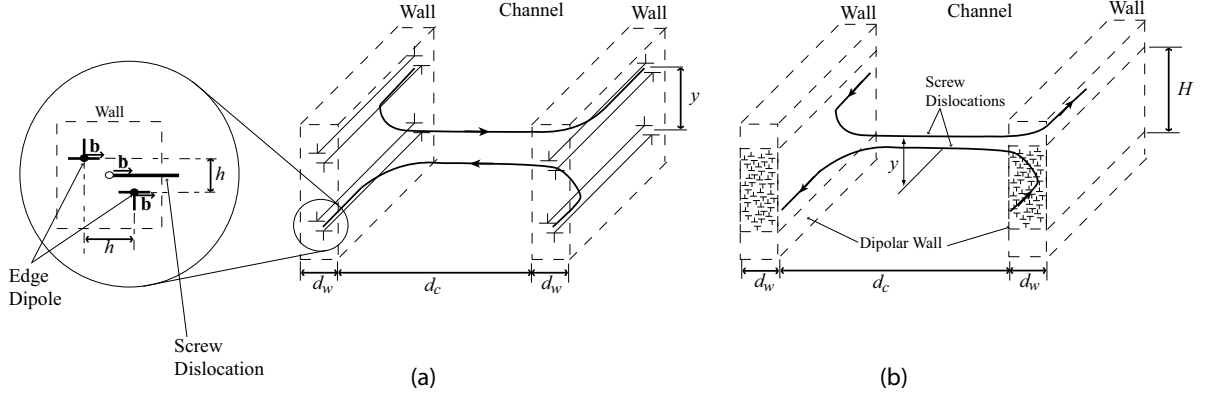


Figure 1: Two PSB models used for the present analysis: (a) only the infinitely long edge dipoles bounding the screw segments on either side of the wall are considered; and (b) a portion of height  $H$  of the dipolar wall with randomly distributed, infinitely-long dipoles is considered.

For all the following analysis, the channel width is denoted by  $d_c$ , the wall thickness is  $d_w$ , the height and width of an edge dipole is  $h$ . The two edge dislocations making up each dipole are inclined at  $45^\circ$ . The spacing between the two slip planes of the screw dislocations is  $y$ . Both the screw dislocations and the edge dipoles in the PSB walls have a Burgers vector,  $\mathbf{b}$ , that is perpendicular to the wall panes. In the present analysis, the edge dipoles are infinitely long, stationary and are not free to expand. Although cross-slip may limit the stability of the screw dipoles, it is not considered in our current model.

As a first approximation, only edge dipoles, which bound the screw segments on either side will be included in the analysis. Thus, as shown in Figure 1-a, each wall is represented by only two infinitely long edge dipoles that are positioned in the middle of the PSB wall. Each dipole is positioned such that the slip plane of one of the screw dislocations passes in the middle between the two edge dislocations forming the edge dipole. This model will be used to study the following effects on the passing stress: (i) the configuration of the two screw dislocations as a result of bowing as they meet and lock as a screw dipole, (ii) the channel width, and (iii) the slip plane separation distance.

In the second model, a portion of height  $H$  of the PSB walls that are densely-packed with edge dislocation dipoles will be considered. As shown in Figure 1-b, each wall is considered to have a density,  $\rho_w$ , of randomly distributed infinitely long edge dipoles. This model will be used to study the effect of the internal stress generated by PSB dipolar walls on dislocation motion inside PSB channels.

In this study, for the numerical simulation of the motion and the interactions of dislocations, we utilize the parametric dislocation dynamics (PDD) method using the DeMecha

code [16]. The PDD method is described with sufficient details in Refs. [13, 14, 17]. In this code, dislocation loops are discretized into curved parametric segments and the stress field everywhere is obtained as a fast numerical quadrature sum [14]. The Peach - Kohler force is then obtained on any other segment point as:  $F_{PK} = \sigma \cdot \mathbf{b} \times \mathbf{t}$  while the self-force is obtained from the local curvature at the point of interest. The variational form of the governing equation of motion (EOM) of a single dislocation loop is given by:  $\int_{\Gamma} (F_k^t - B_{\alpha k} V_{\alpha}) \delta r_k |\mathbf{ds}|$ , where,  $F_k^t$  are the components of the resultant force, consisting of the Peach - Koehler force (generated by the sum of the external and internal stress fields) and the self-force  $F_s$ ,  $B_{\alpha k}$  is the resistivity matrix (inverse mobility),  $V_{\alpha}$  are the velocity vector components, and the line integral is carried along the arc length of the dislocation  $\mathbf{ds}$  [13]. The equations of motion (EOM) of the system of dislocation loops is then solved numerically to update the generalized coordinates and hence determine the new dislocation shapes. After solving the EOM using numerical integration methods, the dislocation shape and position is updated, thus capturing microstructure evolution.

In the present analysis we use the following parameters for copper: the shear modulus  $G = 42.0 \times 10^9$  MPa, the Poisson's ratio  $\nu = 0.31$ , and the magnitude of the Burgers vector  $b = 0.25$  nm.

## Results of Numerical Simulations

Using the model shown in Figure 1-a, the effective resolved shear stress in the middle of the channel as well as the screw dislocation configuration as it expands in the channels are computed and shown in Figure 2. The break up of the total stress into a bowing stress component and a dipolar interaction stress component are shown as well. The glide plane spacing and the channel width for the shown results are kept constant at  $y = 50.0$  nm and  $d_c = 1.2 \mu\text{m}$ , respectively, in agreement with the reported parameters [4, 7]. The results shown are for two distinct cases. In the first case, Figure 2-a, at the beginning of the simulations the two screw dislocations are initially straight and positioned on top of each other. It is clear in this case that the dipolar interactions stress is the dominant factor affecting the passing stress. The two screw dislocations form a dipole at the beginning (step 1), and as the stress increases and reaches a maximum value,  $\tau_{pass}$ , the dipole is broken and the two screw dislocations pass each other (step 2) and start bowing out in the channel until they reach their maximum bowed out configurations (step 3). The two dislocations further propagate with this constant configuration as long as they do not encounter other obstacles (steps 4 & 5).

The passing stress as computed for this case is  $\tau_{pass} = 18.84$  MPa and the maximum dipolar interaction stress is  $\tau_{dip} = 16.84$  MPa, while the computed Orowan bowing stress is  $\tau_{bow} = 15.3$  MPa. It is seen that the calculated passing stress is 19% greater than the Orowan bowing stress. Based on these computed values, if the linear superposition method [3 - 6] is used, the predicted passing stress would be about 32.14 MPa, thus having an over-estimate of 71% from our calculations. In view of this result it is fair to say that Mughrabi and Pschenitzka's [7] passing stress estimate of being about 20% larger than either the screw dipole passing stress or the critical Orowan stress is in good agreement with the current calculations.

In the second case, Figure 2-b, the screw dislocations at the beginning of the simulations are straight and positioned  $1.0 \mu\text{m}$  from each other on their respective glide planes. Initially the two screw dislocations are free to expand in the channel (step 1) without feeling the field

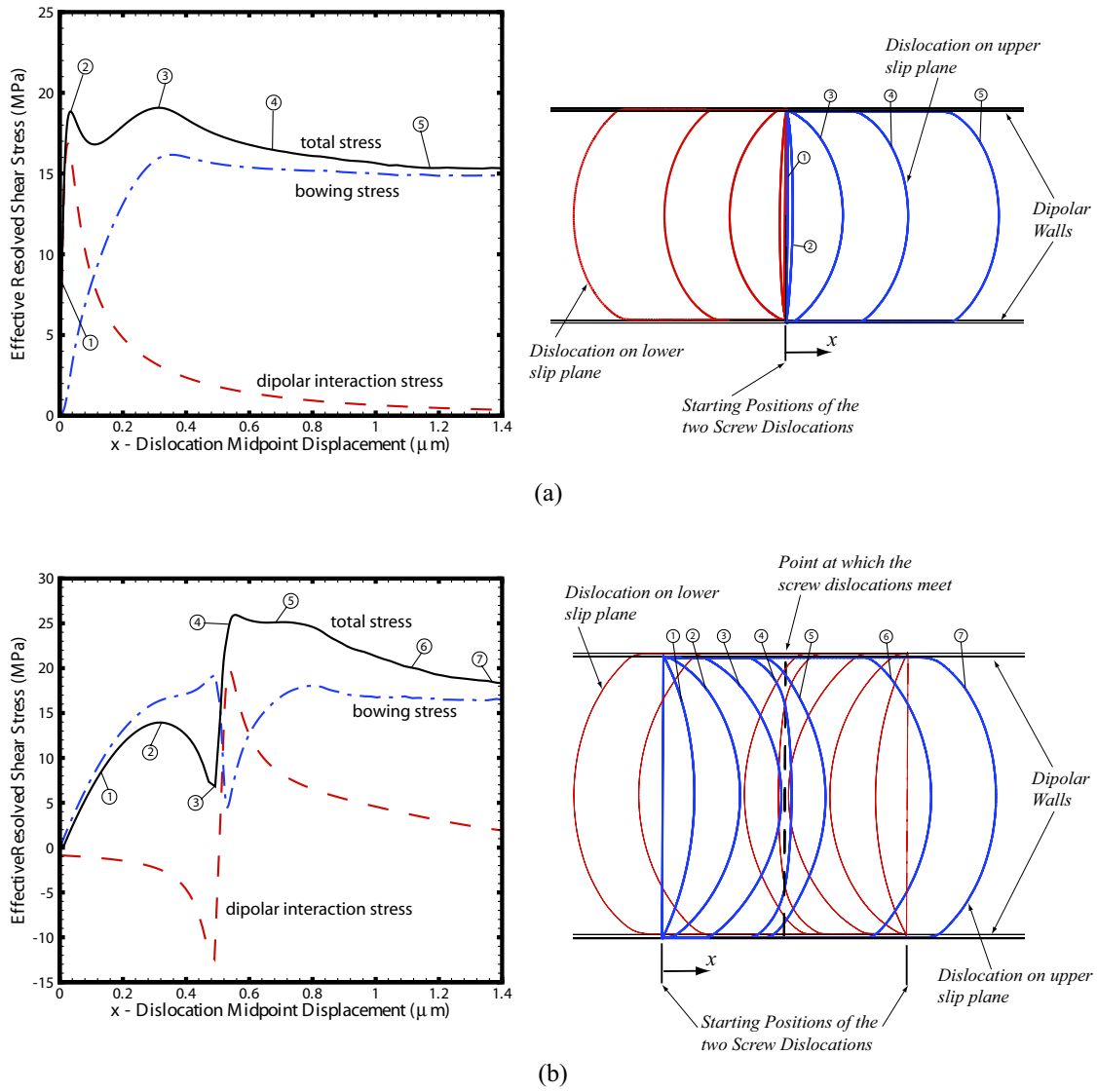


Figure 2: The plots on the left show the effective resolved shear stress (solid line) in the middle of the channel and the break up of its components: the dipolar interaction stress (dashed line), and the bowing stress (dash dot line). The plots on the right show the dislocation configuration as it expands in between the channels where the circled numbers refers to dislocation configuration shown on the left plot. The glide plane spacing and the channel width are kept constant at  $y = 50.0\ \text{nm}$  and  $d_c = 1.2\ \mu\text{m}$  respectively. The two screw dislocations are initially straight and located (a) above each other; (b) separated by  $1\ \mu\text{m}$  from each other on their respective glide planes.

of each other until they reach a maximum bowed out configuration (step 2). After that, the two screw dislocations start feeling the field of each other (step 3) and eventually straighten out in the middle of the channel and form a dipole (step 4). As the applied stress increases to a maximum value,  $\tau_{pass}$ , the dipole configuration is broken and the two screw dislocations pass each other and the screw dislocations bows out again (step 5) and propagate with a constant configuration in the channel(steps 6 & 7).

For this case, the computed passing stress is  $\tau_{pass} = 26.0$  MPa and the maximum dipolar interaction stress is found to be  $\tau_{dip} = 19.8$  MPa, while the computed Orowan bowing stress is  $\tau_{bow} = 16.5$  MPa. Based on these computed values, if the linear superposition method is used, the predicted passing stress would be about 36.6 MPa, thus having an overestimate of 40% from our calculations. In addition, if Brown's method [3] is used, then 37% Orowan bowing stress adds to the passing stress. In view of this result, the current prediction is close to the lower bound of the latest estimate by Brown [3].

In addition, by considering the numerical analysis presented by Schwarz and Mughrabi [8] for the same parameters, they report a passing stress of  $\tau_{pass} = 30.2$  MPa, maximum dipolar interaction stress  $\tau_{dip} = 16.7$  MPa, and a computed Orowan bowing stress  $\tau_{bow} = 18.2$  MPa. It is apparent for their results, when using Brown's prediction [3], 74% of the Orowan bowing stress adds to the passing stress. Thus, Schwarz and Mughrabi [8] prediction is close to the upper bound of the estimate by Brown [3].

The small differences between the present results and those given by Schwarz and Mughrabi [8] apparently lie in the boundary conditions enforced on the gliding dislocations. The addition of edge dipoles to confine the screw dislocations in our model results in a higher curvature of the screw dislocation near the wall and thus the effect of bowing of the screw dislocations is smaller than the case of Schwarz and Mughrabi [8]. The effect of the edge dipoles in the walls on the passing stress will be later discussed in more details.

Although the numerical results of by Křiřt'an and Kratochvil [9], which predicts that about 50-70% of the Orowan bowing stress adds to the passing stress agrees more with Brown [3], it should be noted that the bowing stress in their model is computed from the line tension only, which predicts higher bowing stresses. At the same time, the screw dislocations in their model are confined by a single edge dipole on each side lowering the Orowan bowing stress adds to the passing stress. Thus, Křiřt'an and Kratochvil [9] predict passing stresses that are in between our current predictions and those of Schwarz and Mughrabi [8].

From these results it is apparent that the shape of the screw dislocations as they bow out between the walls and pass one another have an effect on the predicted passing stress. Figure 3 shows the effect of the distance between the two approaching screw dislocations, or in other words, the effect of the bowing of the screw dislocations on the effective resolved shear stress,  $\tau_{eff}$ , in the middle of the channel. The glide plane spacing and the channel width are kept constant at  $y = 50.0$  nm and  $d_c = 1.2$   $\mu$ m respectively. The different lines are for different dislocation starting positions, where the two limiting cases are: (i) the lower limit (solid line) where the two screw dislocations at the beginning of the simulations are straight and located above each other (i.e. a small effect due to the bowing of the screw dislocations); and (ii) the upper limit (dotted line) where the two screw dislocations at the beginning of the simulations are located 1.25  $\mu$ m from each other, thus the screw dislocations bow out completely in the channels before feeling the field of each other (i.e. a big effect due to the bowing of the screw dislocations). The other lines in between are for different cases

that have a mixed affect of bowing and interaction. From the calculations it is apparent that the passing stress can be predicted to be in the following range:  $18.84 \text{ MPa} \leq \tau_{pass} \leq 26.16 \text{ MPa}$ , thus, the Mughrabi and Pschenitzka predict the lower limit for the passing stress while Brown predicts the upper limit.

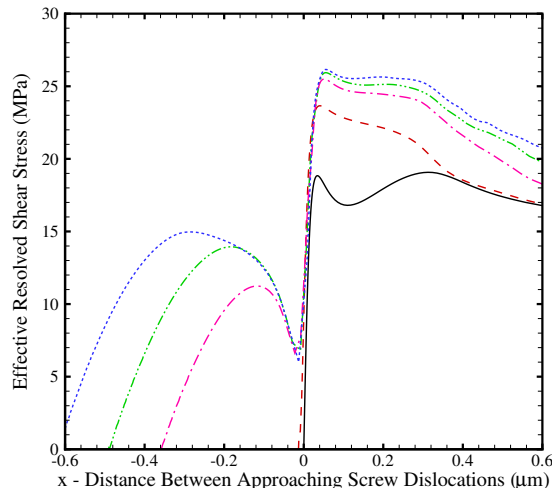


Figure 3: The effect of screw dislocation bowing on the effective resolved shear stress in the middle of the channel. The glide plane spacing and the channel width are kept constant at  $y = 50.0 \text{ nm}$  and  $d_c = 1.2 \text{ }\mu\text{m}$ , respectively. Solid line: screw dislocations are initially above each other; dashed line: screw dislocations are initially  $0.25 \text{ }\mu\text{m}$  from each other; dot-dashed line: screw dislocations are initially  $0.75 \text{ }\mu\text{m}$  from each other; dot-dot-dashed line: screw dislocations are initially  $1.0 \text{ }\mu\text{m}$  from each other; dotted line: the screw dislocations are initially  $1.25 \text{ }\mu\text{m}$  from each other (dotted line).

### Effects of the Internal Stress within the PSB Channel

The local value of the internal stress within the PSB channel is not exactly the same as the applied and resolved shear stress. The local value is changed due to: (i) internal stresses generated by the collective field of edge dipoles in PSB walls; and (ii) the inhomogeneity of the effective elastic properties of the walls and channels. We will address here the influence of the first aspect on the internal stress. Using the model shown in Figure 1-b, a portion of height  $H$  of the densely-packed edge dislocation dipoles is considered. Each wall is considered to have a density,  $\rho_w$ , of randomly distributed infinitely long edge dipoles. In the current analysis, the walls are considered to be rigid.

The effect of the edge dislocation dipole density in the walls,  $\rho_w$ , on the effective resolved shear stress,  $\tau_{eff}$ , in the middle of the channel for both the lower limit condition (the screw dislocations are initially straight and above each other) and the upper limit condition (the screw dislocations are initially straight and  $1.25 \text{ }\mu\text{m}$  from each other) are shown in Figure 4. The glide plane spacing, the channel width, and the average wall thickness are kept constant at  $y = 50.0 \text{ nm}$ ,  $d_c = 1.2 \text{ }\mu\text{m}$ , and  $d_w = 0.1 \text{ }\mu\text{m}$  respectively to be in agreement with experimental observations of PSBs in copper in the steady state condition [4].

Figure 5 shows the effect of the edge dislocation dipole density in the walls on the passing configuration of the screw dislocations. It is clear that by taking a larger portion of the walls into account, and/or increasing the density of the edge dislocation dipoles, will result in reducing the passing stress  $\tau_{pass}$ . When the density of edge dislocations comprising wall dipoles is increased to  $\rho_w = 4.4 \times 10^{15} \text{ m}^{-2}$  for a height  $H = 0.3 \mu\text{m}$ , the passing stress drops by 10% for the lower limit and about 11.6% for the upper limit case. In addition, increasing the density of edge dipoles in the walls increases the curvature of the screw dislocation near the walls, thus, limiting the bowing out of screw dislocations in the channels. It should be noticed that, in experiment observations, the smallest dipole wall height is found to be on the order of  $1 \mu\text{m}$ .

It should be noticed that the maximum drop possible in the passing stress for the lower case is about 11% while for the upper limit case is about 23%. This is because the walls mainly affect the curvature of the screw dislocations near the wall thus decreasing the bowing out of the screws while the dipole interaction stress is not affected. Thus, even if the full wall of  $1 \mu\text{m}$  or more is modelled, the upper limit might be decreased to a value of not less than about 20 MPa.

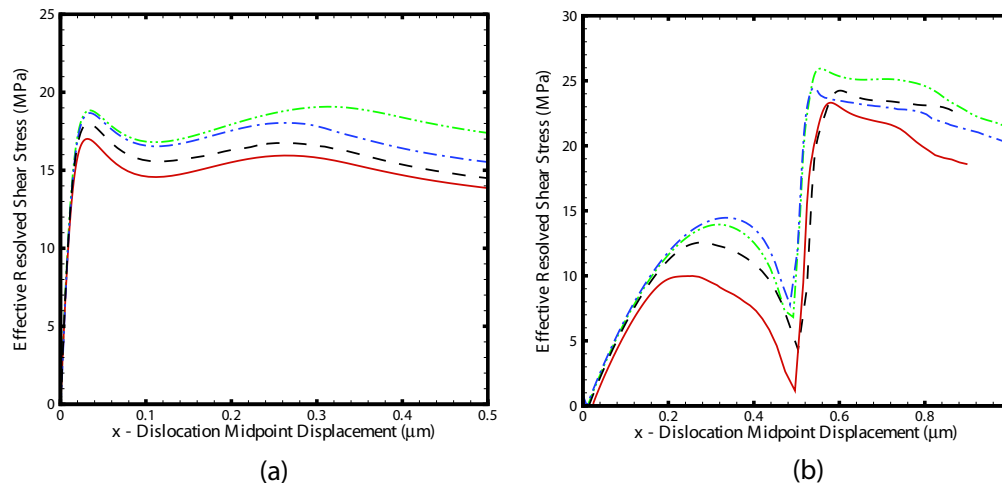


Figure 4: The effect of the edge dislocation dipole density in the walls on the effective resolved shear stress in the middle of the channel. The glide plane spacing and the channel width are kept constant at  $y = 50.0 \text{ nm}$  and  $d_c = 1.2 \mu\text{m}$  respectively. The wall thickness is  $0.1 \mu\text{m}$  and the two screw dislocations are initially straight. (a) The screw dislocations are initially located above each other, and (b) the screw dislocations are  $1.25 \mu\text{m}$  from each other. Dash-dot-dot line: only the edge dipoles bounding the screw segments on either side of the wall are considered in the calculations. dash-dot line:  $\rho_w = 4.4 \times 10^{15} \text{ m}^{-2}$  and  $H = 0.1 \mu\text{m}$ ; dashed line:  $\rho_w = 1.0 \times 10^{16} \text{ m}^{-2}$  and  $H = 0.1 \mu\text{m}$ ; Solid line:  $\rho_w = 4.4 \times 10^{15} \text{ m}^{-2}$  and  $H = 0.3 \mu\text{m}$ .

In Figure 6 the effect of glide plane spacing on the effective resolved shear stress in the middle of the channel for both limiting cases are shown. For this analysis, only edge dipoles bounding screw segments on either side of the wall are considered and the channel width is kept constant at  $d_c = 1.2 \mu\text{m}$ . It is clear from the shown results that the passing stress decreases rapidly with increasing slip plane separation,  $y$ .



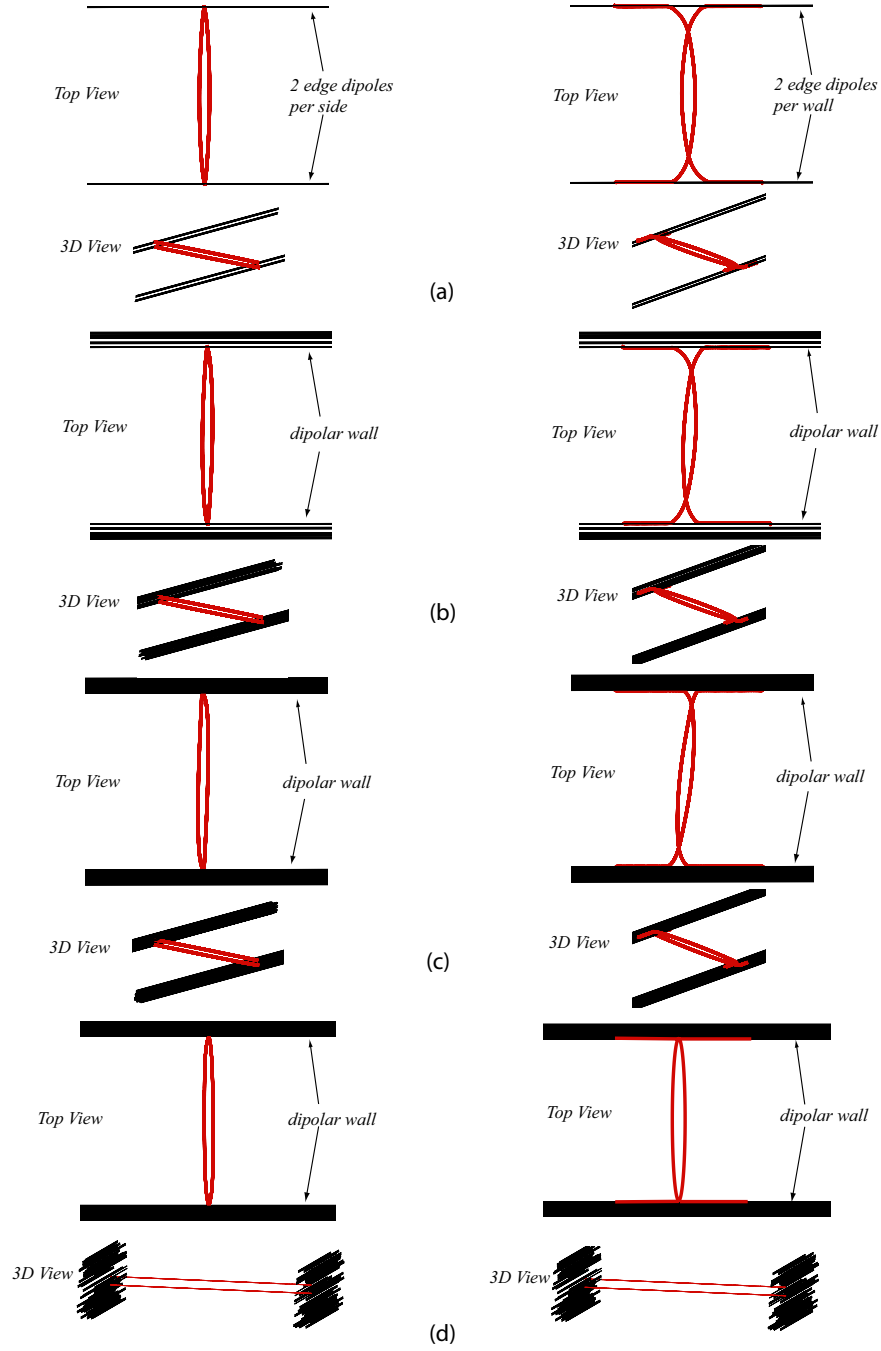


Figure 5: The effect of the edge dislocation dipole density in the walls on the passing configuration of the screw dislocations. The glide plane spacing and the channel width are kept constant at  $y = 50.0$  nm and  $d_c = 1.2$   $\mu\text{m}$ , respectively. The wall thickness is  $0.1$   $\mu\text{m}$  and the two screw dislocations are initially straight. (a) Only the edge dipoles bounding the screw segments on either side of the wall are considered; (b)  $\rho_w = 4.4 \times 10^{15}$   $\text{m}^{-2}$  and  $H = 0.1$   $\mu\text{m}$ ; (c)  $\rho_w = 1.0 \times 10^{16}$   $\text{m}^{-2}$  and  $H = 0.1$   $\mu\text{m}$ ; (d)  $\rho_w = 4.4 \times 10^{15}$   $\text{m}^{-2}$  and  $H = 0.3$   $\mu\text{m}$ .

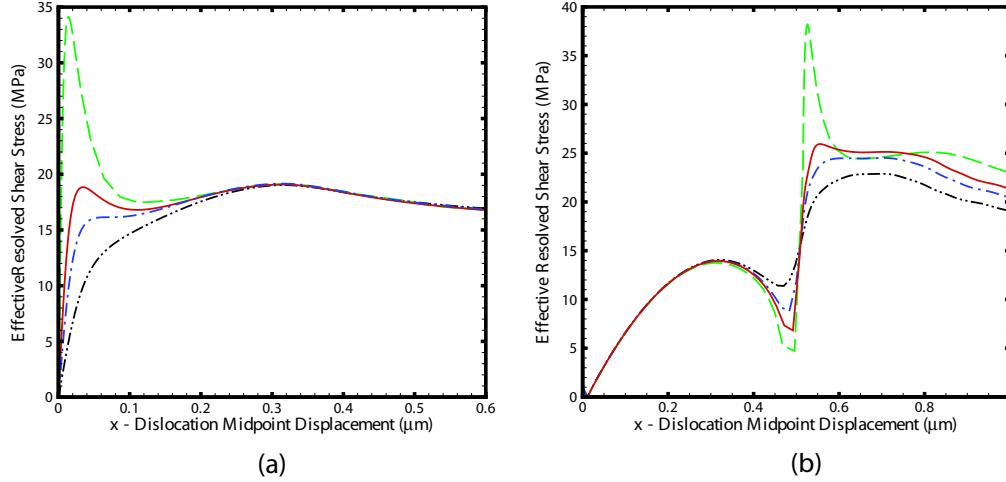


Figure 6: The effect of glide plane spacing on the effective resolved shear stress,  $\tau_{eff}$ , in the middle of the channel for both cases of (a) both screw dislocations are initially above each other; and (b) the screw dislocations are initially  $1.25 \mu\text{m}$  from each other. Only the edge dipoles bounding the screw segments on either side of the wall are considered in the calculations and the channel width is kept constant at  $d_c = 1.2 \mu\text{m}$ . Dashed line:  $y = 25.0 \text{ nm}$ ; solid line:  $y = 50.0 \text{ nm}$ ; dash-dot line:  $y = 65.0 \text{ nm}$ ; dash-dot-dot line:  $y = 100.0 \text{ nm}$ .

Finally, Figure 7 shows the effect of channel width on the effective resolved shear stress in the middle of the channel for the lower limit and upper limit conditions. Only the edge dipoles bounding the screw segments on either side of the wall are considered and the glide plane spacing is kept constant at  $y = 50 \text{ nm}$ .

## Conclusions

A summary of the passing stress results in the present investigation is shown in Figure 8. Details of the shape of the screw dislocations as they simultaneously bow out in between the walls are seen to have a considerable effect on the passing stress, thus validating the need for accurate DDD simulations. From a comparison between the current numerical results and previous published analytical models, it is seen that the results presented by Mughrabi and Pschenitzka [7] give a lower limit for the passing stress while the results presented by Brown [3] give an upper limit.

In addition, the long range internal stress field in the edge dislocation dipolar walls is seen to have an effect on the passing stress as well. It follows that the passing stress in the middle of the channel is reduced to the following limits:  $16.8 \leq \tau_{pass} \leq 20 \text{ MPa}$  which is in agreement with the well-established fact that the stress acting locally in the channels of the heterogeneous PSB structure are modified markedly from the macroscopically applied value by long-range internal stresses [2, 6, 7, 8]. In fact it is reported that the stress acting locally in the channel is lowered to about 16 to 17 MPa [2, 7], which is in reasonable agreement with the current numerical predictions.

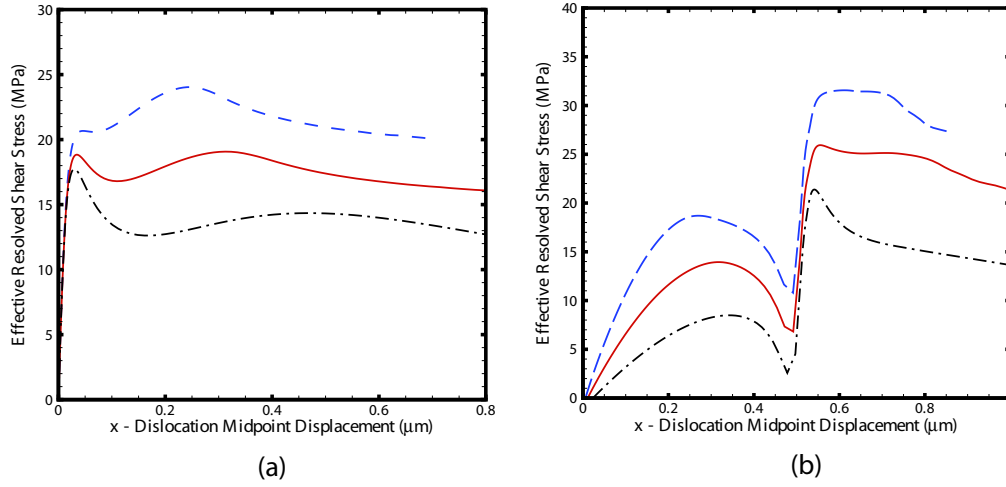


Figure 7: The effect of channel width on the effective resolved shear stress in the middle of the channel for both cases of (a) both screw dislocations are initially above each other; and (b) the screw dislocations are initially  $1.25 \mu\text{m}$  from each other. Only the edge dipoles bounding the screw segments on either side of the wall are considered in the calculations and the glide plane spacing is kept constant at  $y = 50 \text{ nm}$ . Dashed line:  $d_c = 0.95 \mu\text{m}$ ; solid line:  $d_c = 1.2 \mu\text{m}$ ; dash-dot line:  $d_c = 1.6 \mu\text{m}$ .

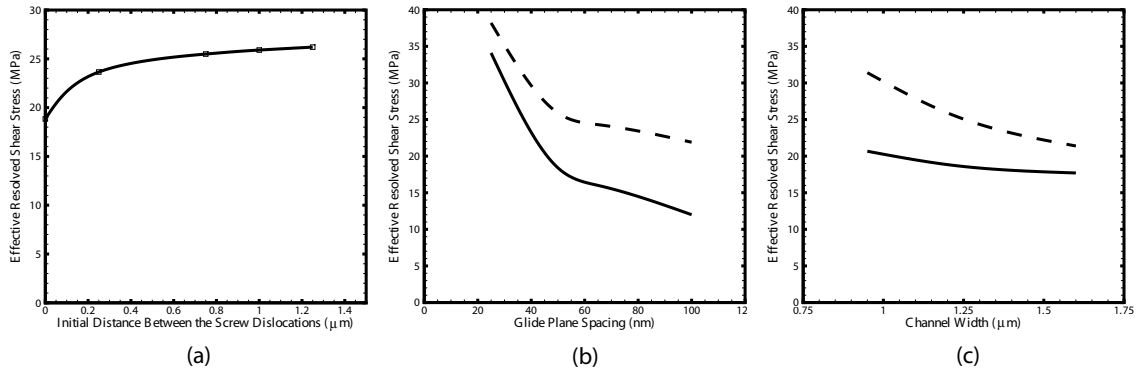


Figure 8: Passing stress (Maximum applied resolved shear stress) as a function of: (a) initial distance between the screw dislocations; (b) glide plane spacing; (c) channel width. In (b) and (c) the solid line represents the case where the two screw dislocations are initially on top of each other while the dashed line represents the case where the two screw dislocations are initially separated by  $1.25 \mu\text{m}$ .

## Acknowledgements

J.A. El-Awady and N.M. Ghoniem would like to acknowledge the support of the U.S. National Science Foundation (NSF) for this research, through Grant No. DMR-0113555, and the support of the U.S. Air Force Office for Scientific Research (AFOSR), through Grant No. F49620-03-1-0031, with UCLA.

## References

- [1] U. Essmann, U. Gösele, and H. Mughrabi. A Model of Extrusions and Intrusions in Fatigued Metals: (I) Point-Defect Production and Growth of Extrusions. *Phil. Mag. A*, 44 (2)(1981), 405–426.
- [2] H. Mughrabi. The Long-Range Internal Stress Field in the Dislocation Wall Structure of Persistent Slip Bands. *phys. stat. sol. (a)*, 104(1987), 107–120.
- [3] L. Brown. Dislocation Bowing and Passing in Persistent Slip Bands. *Phil. Mag.*, 86 (25-26)(2006), 4055–4068.
- [4] J.C. Grosskreutz and H. Mughrabi. "Description of the Work-Hardend Structure at Low Temperature in Cyclic Deformation" in *Constitutive Equations in Plasticity*, edited by A.S. Argon (Cambridge, Mass, MIT Press) p. 251, 1975.
- [5] L. Brown. Dislocation Plasticity in Persistent Slip Bands. *Mater. Sci. Eng.*, A285 (2000), 35–42.
- [6] L. Brown. A Discussion of the Structure and Behaviour of Dipole Walls in Cyclic Plasticity. *Phil. Mag.*, 42 (24)(2004), 2501–2520.
- [7] H. Mughrabi and F. Pschenitzka. Constrained Glide and Interaction of Bowed-Out Screw Dislocations in Confined Channels. *Phil. Mag.*, 85 (26–27)(2005), 3029–3045.
- [8] K. W. Schwarz and H. Mughrabi. Interaction and Passing Stress of Two Threading Dislocations of Opposite Sign in a Confined Channel. *Phil. Mag. Letters*, submitted, 2006.
- [9] J. Křišť'an and J. Kratochvil. Interaction of Glide Dislocations in a Channel of a Persistent Slip Band. *Phil. Mag.*, to be submitted (2006).
- [10] L. P. Kubin, G. Canova, M. Condat, B. Devincre, V. Pontikis, and Y. Brechet. *Diffusion and Defect Data - Solid State Data, Part B (Solid State Phenomena)*, 23-24(1992), 455.
- [11] R. M. Zbib, M. Rhee, and J. P. Hirth. *In. J. Mech. Sci.*, 40 (2-3)1998, 113.
- [12] K.W. Schwarz. Simulation of Dislocations on the Mesoscopic Scale. *J. Appl. Phys.*, 85 (1999), 108–129.
- [13] N. M. Ghoniem, S.-H. Tong, and L. Z. Sun. Parametric Dislocation Dynamics: A Thermodynamics-Based Approach to Investigations of Mesoscopic Plastic Deformation. *Phys. Rev.*, 61 (2)(2000), 913–927.
- [14] N. M. Ghoniem and L. Z. Sun. Fast Sum Method for the Elastic Field of 3-D Dislocation Ensembles. *Phys. Rev.*, 60 (1)(1999), 128–140.

- [15] S. Gavazza and D. Barnett. The Self-Force on a Planar Dislocation Loop in an Anisotropic Linear-Elastic Medium. *J. Mech. Phys. Solids*, 24(1999), 171–185.
- [16] Z. Wang, N. M. Ghoniem, S. Swaminarayan, and R. LeSar. A Parallel Algorithm for 3D Dislocation Dynamics. *J. Comp. Phys.*, In Press (2006).
- [17] N. M. Ghoniem, J. Huang, and Z. Wang. Affine Covariant-Contravariant Vector Forms for the Elastic Field of Parametric Dislocations in Isotropic Crystals. *Phil. Mag. Lett.*, 82(2)(2002), 55-63.